

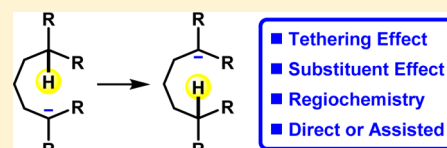
# Carbanion Translocations via Intramolecular Proton Transfers: A Quantum Chemical Study

Yi Wang, Pei-Jun Cai, and Zhi-Xiang Yu\*<sup>✉</sup>

Beijing National Laboratory for Molecular Sciences (BNLMS), Key Laboratory of Bioorganic Chemistry and Molecular Engineering of Ministry of Education, College of Chemistry, Peking University, Beijing 100871, China

**S** Supporting Information

**ABSTRACT:** Intramolecular proton transfers are important processes in chemical reactions and biological transformations. In particular, the translocation of reactive carbanion centers can be achieved through  $1,n$ -proton transfer in either a direct or an assisted manner (via the protonation/deprotonation mechanism). Despite some mechanistic investigations on proton transfers within zwitterionic species, no guiding principles have been summarized for carbanion-induced intramolecular proton transfers. Herein, we report our quantum chemical study on the carbanion translocations via intramolecular proton transfers. Our calculations indicated that the reaction barriers generally decrease with longer tether lengths and more  $\pi$ -withdrawing substituents. The physical bases behind these effects were revealed according to the charge and bond energy decomposition analysis, showing that the destabilizing closed-shell Pauli repulsions play important roles in determining the relative ease of intramolecular proton transfers. We also found that the thermodynamic driving force may affect the regiochemistry. This study may help chemists to understand whether a carbanion translocation occurs via an intramolecular proton transfer or with the assistance of proton shuttles, such as water and alcohols.



## INTRODUCTION

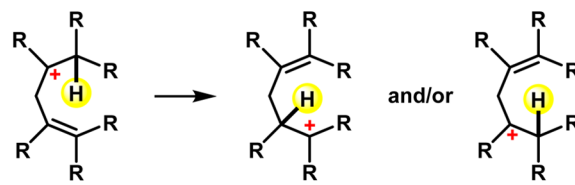
Intramolecular hydrogen transfer is one of the most fundamental processes in chemical and biological reactions.<sup>1–5</sup> In organic chemistry, intramolecular hydrogen transfer between carbon atoms is of extreme importance because the translocation of the reactive carbon centers, such as carbocations,<sup>1,6–8</sup> carboradicals,<sup>2</sup> and carbanions,<sup>9–13</sup> might be accompanied by the cleavage of inert carbon–hydrogen bonds.<sup>14</sup> While the intramolecular hydride<sup>1</sup> and hydrogen atom transfers<sup>2</sup> have been well studied both experimentally and computationally, intramolecular proton transfers between carbons have been much less investigated.<sup>6–13</sup>

To date, two types of intramolecular carbon-to-carbon proton transfers have been discovered (Scheme 1).<sup>15</sup> The first one is the intramolecular proton transfer from a carbocation to a carbon–carbon double bond (Scheme 1a),<sup>6–8</sup> which was first proposed to explain the hydrogen migrations in terpene biosynthesis.<sup>6</sup> In 2008, Surendra and Corey carried out labeling experiments to confirm that an intramolecular carbocation translocation can proceed through a direct 1,5-proton transfer.<sup>7</sup> Recently, Hong and Tantillo summarized the previous reports<sup>6,7</sup> in this area and listed five guiding principles to predict the feasibility of carbocation translocations via intramolecular proton transfers in terpene biosynthesis.<sup>8</sup>

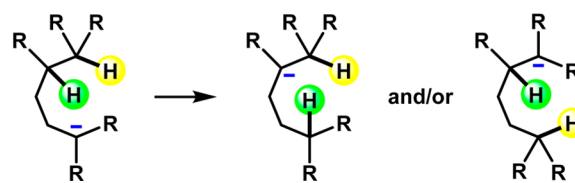
The other type of intramolecular carbon-to-carbon proton transfer is initiated by carbanion species (Scheme 1b).<sup>9–13</sup> Due to the fact that the generation of free carbanions in solution is difficult,<sup>16,17</sup> to date, only a few examples of carbanion translocations in zwitterionic species were discussed, including

## Scheme 1. Two Types of Intramolecular Carbon-to-Carbon Proton Transfers

### (a) Proton transfers to alkenes (refs 6–8)



### (b) Proton transfers to carbanions (this work)



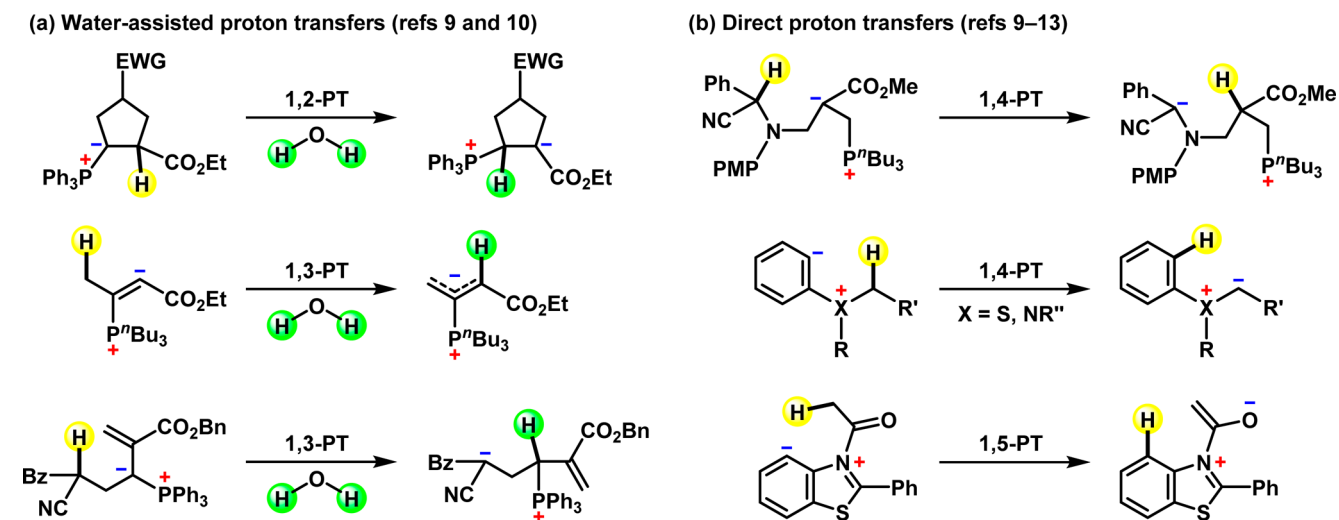
phosphine-catalyzed<sup>9,10</sup> and aryne-mediated<sup>11–13</sup> transformations (Scheme 2).

Previously our computational and experimental studies indicated that the 1,2- and 1,3-proton transfers in phosphine-catalyzed (3 + 2) cycloadditions first reported by Lu and co-workers<sup>9a</sup> are not concerted, but assisted by water (Scheme 2a, top and middle).<sup>10a–d</sup> The Tong group also found that the 1,3-proton transfer in their phosphine-catalyzed (4 + 1) cycloaddition may occur through an intermolecular process (Scheme 2a, bottom).<sup>9d</sup> However, recently Wei, Qiao, and co-workers<sup>10f</sup>

Received: January 25, 2017

Published: April 17, 2017

Scheme 2. Selected Examples for Carbanion Translocations via Proton Transfers



found that the 1,4-proton transfer may occur intramolecularly during their computational study on the phosphine-catalyzed intramolecular Michael addition discovered by the Liao group (Scheme 2b, top).<sup>9c</sup> Similarly, the 1,4-proton transfers in the generations of sulfur and nitrogen ylides induced by the additions of thioethers, amines, imines, and aziridines to arynes were proposed to proceed through intramolecular processes (Scheme 2b, middle).<sup>12</sup> Moreover, 1,5-proton transfer induced by an aryl anion may also take place intramolecularly according to the deuterium labeling studies by Li and co-workers in their domino aryne chemistry (Scheme 2b, bottom).<sup>13</sup>

Despite these and other known examples, no guiding principles have been summarized for carbanion-induced intramolecular proton transfer, which is in sharp contrast with those for carbocation-induced intramolecular hydride<sup>1</sup> and proton transfers.<sup>6–8</sup> Therefore, it is important to understand the regiochemistry of these intramolecular proton transfers and whether a carbon-to-carbon proton transfer takes place in a direct or an assisted manner (via the protonation/deprotonation mechanism). These mechanistic insights may help chemists to optimize the reaction conditions and to design new catalysts and synthetic methodologies.

Here we report our quantum chemical study on carbanion translocations via intramolecular proton transfers. The influence of the tether length and the substituent effect on the relative ease of the intramolecular proton transfers was investigated. We also revealed the physical bases behind these effects.

## COMPUTATIONAL METHODS

**Geometry Optimizations with Gaussian 09 Software Package.**<sup>18</sup> Pruned integration grids with 99 radial shells and 590 angular points per shell were used. Geometry optimizations of all the minima and transition structures involved were carried out using the  $\omega$ B97XD functional<sup>19</sup> and the 6-311+G(d,p) basis set<sup>20</sup> without any constraints. Unscaled harmonic frequency calculations at the same level were performed to validate each structure as either a minimum or a transition structure and to evaluate its zero-point energy (ZPE). All conformers were located, but only the most stable ones were reported. We found that the performance of the  $\omega$ B97XD functional in the calculations of thermochemistry and kinetics for intramolecular carbon-to-carbon proton transfers is superior to those of seven other popular density functionals based on a benchmark study against high-level *ab initio* calculations (see Supporting Information for details).

## Energy Refinements Using ORCA 3.0.3 Program System.<sup>21</sup>

Spin-component-scaled second-order Møller–Plesset perturbation theory (SCS-MP2)<sup>22,23</sup> and the aug-cc-pVTZ basis set<sup>24</sup> were used for single-point energy calculations based on the optimized structures at the  $\omega$ B97XD/6-311+G(d,p) level. The convergence thresholds were set to “TIGHTSCF”. Frozen core approximations and the resolution of the identity (RI)<sup>25</sup> using the aug-cc-pVTZ/C auxiliary basis set<sup>26</sup> were used to speed up the correlation calculations.

All discussed energy differences were based on the ZPE-corrected electronic energies at the SCS-MP2/aug-cc-pVTZ// $\omega$ B97XD/6-311+G(d,p) level unless otherwise specified. Gibbs energies of activation and theoretical rate constants for selected reactions were listed in the Supporting Information for reference.

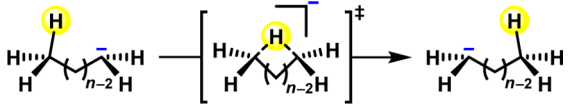
**Bond Energy Decomposition Analysis with Amsterdam Density Functional (ADF) Modeling Suite 2016.106.**<sup>27,28</sup> Bond energy decomposition analysis and the related all-electron DFT calculations were performed using the  $\omega$ B97X functional.<sup>29</sup> The ATZ2P Slater-type orbital (STO) basis set<sup>30</sup> and the corresponding auxiliary set of s, p, d, f, and g STOs were used. The geometry of the intermolecular proton transfer transition structure was optimized in  $D_{3d}$  symmetry. Based on this structure, a potential energy surface (PES) scan was performed by reducing the C⋯H⋯C bond angle from 180° to 90° in steps of 10° with the C⋯H bond lengths maintained, while the remaining geometry parameters were allowed to relax ( $C_2$  symmetry was applied).

3D structures were prepared with CYLview<sup>31</sup> and GUI 2016.<sup>32</sup>

## RESULTS AND DISCUSSION

**Degenerate Intramolecular Proton Transfers in Unsubstituted Primary Carbanions.** We commenced our study with degenerate proton transfers in unsubstituted primary carbanions A–F (Table 1).<sup>33</sup> These reactions are thermoneutral ( $\Delta E_{\text{rxn}} = 0$ ) and, therefore, can be discussed without bias caused by the thermodynamic contributions. The substituent effect will be discussed later.

**1,2-Proton Shift.** According to the selection rules for sigmatropic reactions developed by Woodward and Hoffmann,<sup>34</sup> the concerted (*suprafacial*) 1,2-proton shift is supposed to be thermally symmetry-forbidden.<sup>35</sup> As depicted in Figure 1a, the positive overlap between the SOMO (singly occupied molecular orbital) of the ethylene anion radical and the migrating hydrogen orbital cannot be maintained during the sigmatropic shift. Our quantum chemical calculations indicated that the activation barrier of the direct 1,2-proton shift in ethyl anion A via transition structure TS1 (Figure 1b) is 48.2 kcal/

Table 1. 1,*n*-Proton Transfers within Primary Carbanions<sup>a</sup>


<i>n</i>	carbanion	TS	$\Delta E^\ddagger$
2	ethyl anion, A	TS1	48.2
3	<i>n</i> -propyl anion, B	TS2	34.2
4	<i>n</i> -butyl anion, C	TS3	18.2
5	<i>n</i> -pentyl anion, D	TS4	17.2
6	<i>n</i> -hexyl anion, E	TS5	15.1
7	<i>n</i> -heptyl anion, F	TS6	16.0

<sup>a</sup>Energies are reported in kcal/mol.  $\Delta E_{\text{rxn}} = 0$  in all cases. rxn = reaction.

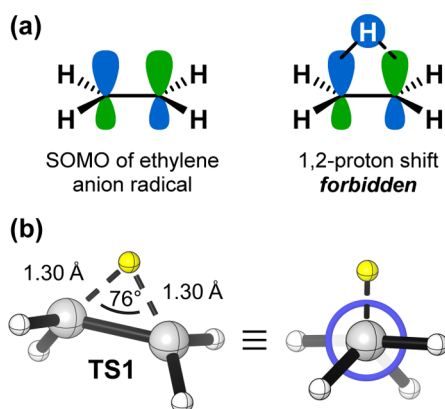


**Figure 1.** (a) Analysis of the *suprafacial* 1,2-proton shift in ethyl anion A according to the Woodward–Hoffmann rules.<sup>34</sup> SOMO = singly occupied molecular orbital. (b) Optimized geometries for the 1,2-proton shift transition structure TS1. Color scheme: C, gray; H, white; the migrating hydrogen, yellow.

mol, which is extremely difficult to overcome under traditional thermal conditions.

**1,*n*-Proton Transfers.** For other primary carbanions, because of the presence of saturated hydrocarbon linkers, the relative ease of the intramolecular proton transfers cannot be guided by the standard Woodward–Hoffmann analysis, which could only be applied to conjugated polyenes and the related charged systems.<sup>34</sup> Therefore, we utilized quantum chemical calculations to investigate these reactions. The computed activation barriers for 1,*n*-proton transfers in simple primary carbanions were plotted in Figure 2a. Selected bond lengths and angles were also summarized and shown in Figure 2b and 2c, respectively. The optimized geometries for the intramolecular proton transfer transition structures can be found in Figure 3.

Interestingly, we observed a monotonic decrease of the activation barriers from *n* = 2 to 6 (Figure 2a). Such a trend was stopped when *n* reached 7. Moreover, we found that when *n* increases, the C⋯H bond length in the 1,*n*-proton transfer transition structure rapidly converges to (1.45 ± 0.01) Å (Figure 2b), whereas, the C⋯H⋯C bond angle converges at a much slower rate (Figure 2c). Based on the different convergence rate of these geometric parameters, we expected that the optimal C⋯H bond length for the transition structure has already been achieved when *n* reaches 3; however, the geometric requirement for the C⋯H⋯C bond angle cannot be satisfied due to the presence of ring strain, especially when *n* is small.

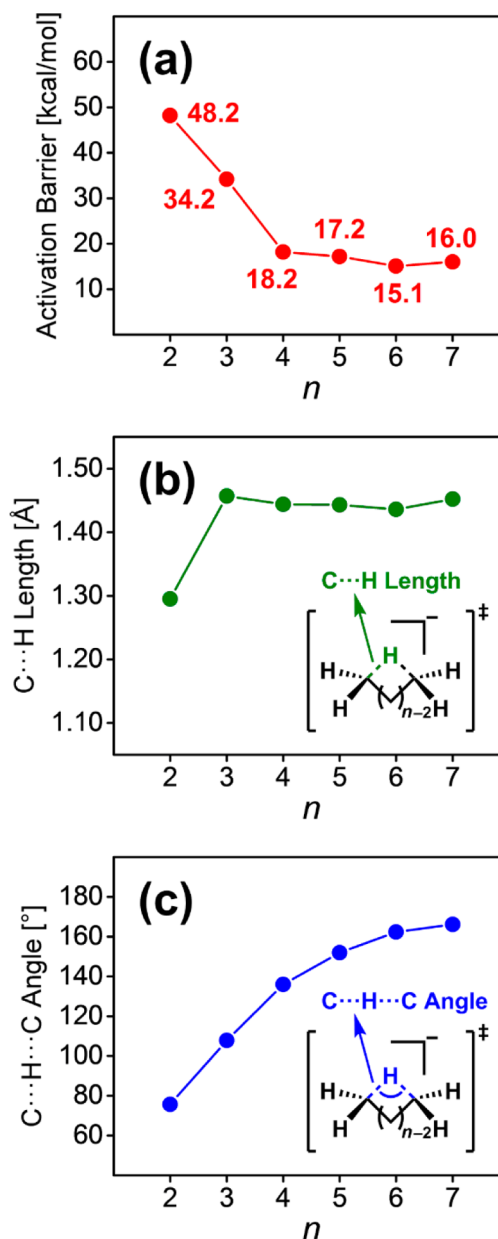


**Figure 2.** Degenerate proton transfers in acyclic primary carbanions A–F. (a) Activation barriers of 1,*n*-proton transfers. (b and c) Selected geometric parameters for 1,*n*-proton transfer transition structures TS1–6.

To understand such a stereoelectronic requirement better, we investigated the intermolecular proton transfer between methane and the methyl anion in which no ring strain exists. In fact, this intermolecular reaction can be regarded as an analog of the 1,*n*-proton transfer within carbanions when *n* approaches infinity. In accordance with the previous computational studies,<sup>36</sup> our calculations at the SCS-MP2// $\omega$ B97XD level also suggested the existence of a double-well potential energy surface (Figure 4). The proton transfer within the weak hydrogen-bonded complex G via TS7 requires overcoming an activation barrier of 11.6 kcal/mol. In the transition structure, the lengths for the breaking and forming C⋯H bonds are both 1.45 Å (Figure 4), which are almost identical to those in the intramolecular cases (Figure 3). This result supported our hypothesis that the geometric requirement for the C⋯H bond

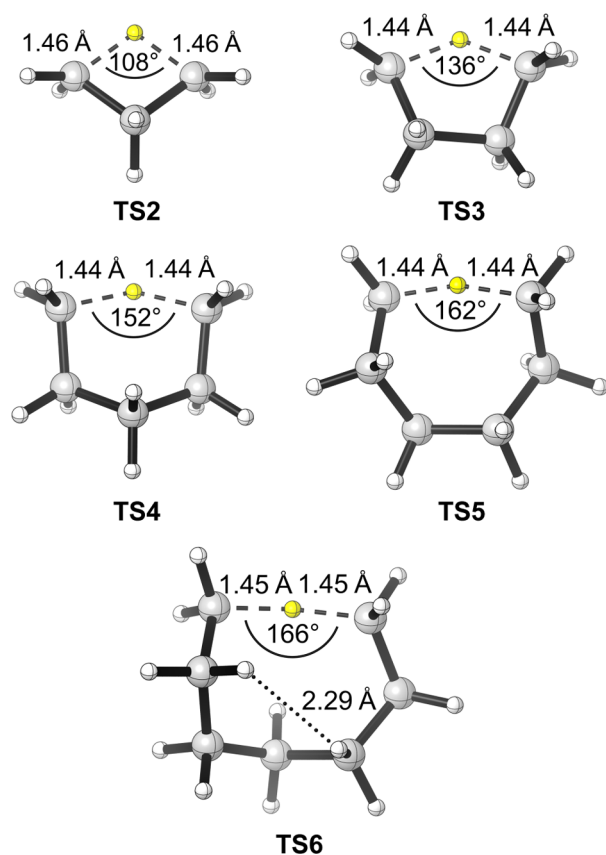


**Figure 3.** Optimized geometries for the intramolecular proton transfer transition structures **TS2–6**. Color scheme: C, gray; H, white; the migrating hydrogen, yellow.

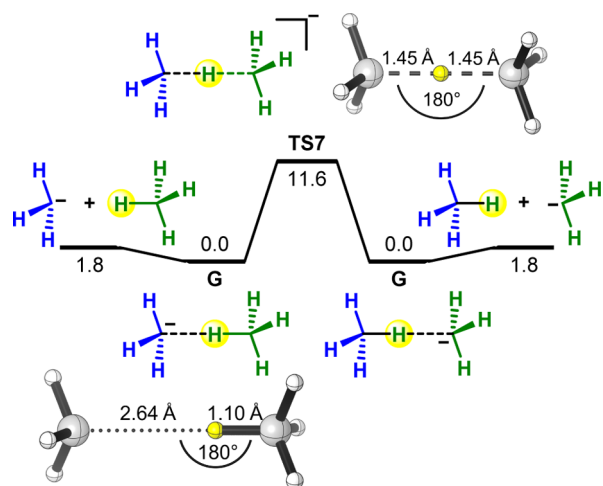


**Figure 4.** Double-well potential energy surface of the intermolecular carbon-to-carbon proton transfer. Energies are reported in kcal/mol. Color scheme: C, gray; H, white; the migrating hydrogen, yellow.

length in the proton transfer transition structure has already been satisfied even with a short tether length, such as  $n$  equals 3 or 4.

Moreover, we found a linear  $C\cdots H\cdots C$  arrangement in **TS7**, corresponding to a  $C\cdots H\cdots C$  bond angle of  $180^\circ$ .<sup>36</sup> In the intramolecular cases, when  $n$  increases, the  $C\cdots H\cdots C$  bond angle converges toward but never reaches  $180^\circ$ . We reasoned that the attempt to achieve a linear  $C\cdots H\cdots C$  arrangement in the transition structure leads to the increase of ring strain

during the  $1,n$ -proton transfer, especially when  $n$  is small. As a result, the  $C\cdots H\cdots C$  structure bends to balance the geometric requirement and ring strain. When  $n$  becomes larger, the penalty from the ring strain will be relatively smaller owing to the presence of more flexible carbon–carbon single bonds, and consequently, the intramolecular proton transfer is easier. However, when  $n$  reaches 7, the proton transfer occurs through an eight-membered-ring transition structure and suffers an additional penalty caused by transannular interactions (Figure 3, bottom), which are common in medium-sized rings.<sup>37</sup>

#### Rationalization of the Linear $C\cdots H\cdots C$ Arrangement in the Intermolecular Proton Transfer Transition Structure.

By far, we have rationalized that the relative ease of  $1,n$ -proton transfer is determined by the trade-off between the ring strain and the geometric requirement for linear  $C\cdots H\cdots C$  arrangement in the transition structure. But, one question still remains: why does the proton transfer transition structure favor a linear structure?

To answer this question, we utilized the ETS–NOCV charge and energy decomposition scheme developed by Ziegler and co-workers,<sup>38</sup> which combines the extended transition structure (ETS) method<sup>39</sup> with the natural orbitals for chemical valence (NOCV) theory.<sup>40</sup> By using this approach, we can decompose the bond energy of the transition structure between the interacting fragments into destabilizing (distortion and Pauli repulsion) and stabilizing (electrostatic and orbital interaction) components.<sup>41</sup>

We considered that the intermolecular proton transfer transition structure **TS7** forms from methane and methyl anion fragments. As shown in Figure 5a, repulsive Pauli interaction causes the decrease of the electron density in the overlap region as judged by the Pauli deformation density. Such a destabilizing interaction of 116.0 kcal/mol mainly comes from the closed-shell HOMO–HOMO interaction between methyl anion and the distorted methane (Figure 5a). ETS–NOCV

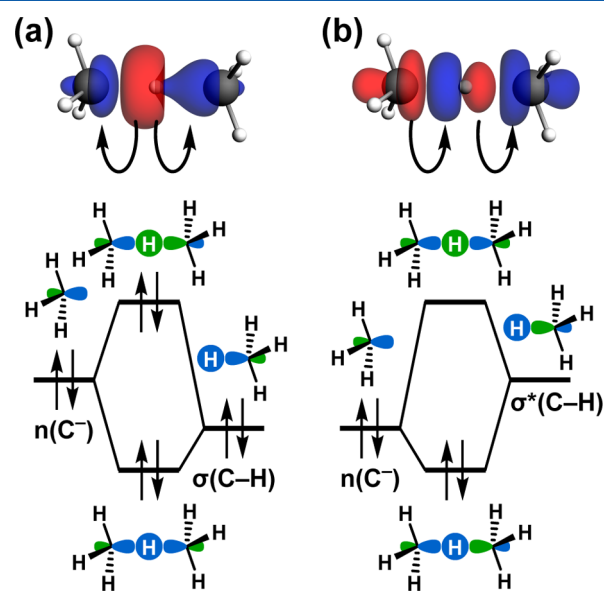


**Figure 5.** Deformation densities and orbital interactions describing (a) Pauli repulsion and (b)  $n(C^-) \rightarrow \sigma^*(C-H)$  interaction in **TS7** formed from methyl anion and methane calculated at the  $\omega$ B97X/ATZ2P level. The arrows indicate the direction of charge transfer. Color scheme: electron density increases ( $\Delta\rho > 0$ ), blue; electron density decreases ( $\Delta\rho < 0$ ), red. Isovalue = 0.005.

Table 2. Analysis of the Interactions between CH<sub>4</sub> and CH<sub>3</sub><sup>-</sup> in [H<sub>3</sub>C⋯H⋯CH<sub>3</sub>]<sup>-</sup> with Different C⋯H⋯C Bond Angles<sup>a</sup>

bond angle	180°	170°	160°	150°	140°	130°	120°	110°	100°	90°
$\Delta\Delta E$	0.0	0.4	1.5	3.4	6.2	10.5	17.2	27.8	45.1	72.4
$\Delta\Delta E_{\text{dis}}(\text{CH}_4)$	0.0	0.2	0.9	2.0	3.3	4.5	5.8	6.0	6.0	6.2
$\Delta\Delta E_{\text{dis}}(\text{CH}_3^-)$	0.0	0.0	0.0	0.0	0.0	0.0	0.1	0.2	0.7	1.8
$\Delta\Delta E_{\text{int}}$	0.0	0.2	0.6	1.4	2.9	6.0	11.3	21.6	38.4	64.4
$\Delta\Delta E_{\text{Pauli}}$	0.0	0.4	1.1	2.5	5.4	11.2	21.1	40.4	73.9	129.8
$\Delta\Delta V_{\text{elstat}}$	0.0	-0.2	-0.6	-1.3	-2.5	-4.7	-8.2	-14.6	-26.0	-45.5
$\Delta\Delta E_{\text{oi}}$	0.0	0.0	0.1	0.2	0.0	-0.5	-1.6	-4.2	-9.5	-19.9

<sup>a</sup>Energies are reported in kcal/mol. Computed at the  $\omega$ B97X/ATZ2P level.  $\Delta\Delta E = \Delta\Delta E_{\text{dis}}(\text{CH}_4) + \Delta\Delta E_{\text{dis}}(\text{CH}_3^-) + \Delta\Delta E_{\text{int}}$ .  $\Delta\Delta E_{\text{int}} = \Delta\Delta E_{\text{Pauli}} + \Delta\Delta V_{\text{elstat}} + \Delta\Delta E_{\text{oi}}$ . dis = distortion. int = interaction. Pauli = Pauli repulsion. elstat = electrostatic. oi = orbital interaction.

analysis also indicated that the stabilization of the transition structure comes from the electrostatic (-51.5 kcal/mol) and donor-acceptor orbital interactions (-83.0 kcal/mol). Figure 5b depicts the leading stabilizing orbital interaction in the proton transfer transition structure. This contribution (-68.0 kcal/mol) is due to the donation of electrons from the HOMO of the methyl anion (mainly  $n(\text{C}^-)$  orbital) into the LUMO of methane (mainly  $\sigma^*(\text{C}-\text{H})$  orbital), corresponding to the traditional thinking of the acid-base chemistry (Figure 5b). Another chemically meaningful component (-9.3 kcal/mol) represents the back-donation from the HOMO of methane into the LUMO of the methyl anion.

Then, we investigated the influence of the decrease of C⋯H⋯C bond angle in the transition structure TS7 on the bond energy (see Computational Methods for details). We also performed ETS-NOCV analysis to shed light on which energy component determines the linear C⋯H⋯C arrangement during the proton transfer (Table 2). As depicted in Figure 6a, the bond energy increases when the C⋯H⋯C bond angle deviates from 180°. The change in the distortion energy of methyl anion is negligible, whereas the distortion energy of methane and the interaction energy give important contributions. Notably, the growth rates of these two components are different (Figure 6b). The distortion energy of methane increases linearly yet becomes a constant after the C⋯H⋯C bond angle reaches 120°, while the interaction energy grows in an exponential manner, which may account for the trend of the total bond energy.

The interaction energy was further decomposed into chemically meaningful terms (Figure 6c). The electrostatic interaction becomes more stabilizing when the C⋯H⋯C bond angle decreases due to the shorter distance between the methane and methyl anion. Therefore, it is not the reason why the proton transfer favors a linear C⋯H⋯C arrangement. One may expect that the stabilizing HOMO-LUMO interactions are more sensitive to the directivity. But our ETS-NOCV study indicated that the decrease in the stabilizing orbital interactions is less than 0.2 kcal/mol due to the fact that the LUMO orbital of methane mainly consists of the 1s orbital of H with spherical symmetry and thus the  $n(\text{C}^-) \rightarrow \sigma^*(\text{C}-\text{H})$  interaction is not very sensitive to the directivity. Moreover, a smaller C⋯H⋯C bond angle induces a shorter distance between the methane and methyl anion and increases the overlap between their frontier orbitals. As a result, the orbital interactions even become more stabilizing than those in TS7 after the C⋯H⋯C bond angle reaches 130°. Finally, only the Pauli repulsion, which originates from the destabilizing HOMO-HOMO interaction, may account for the increasing trend of the bond energy. As shown in Figure 7, there indeed exists a linear correlation between the relative bond energies

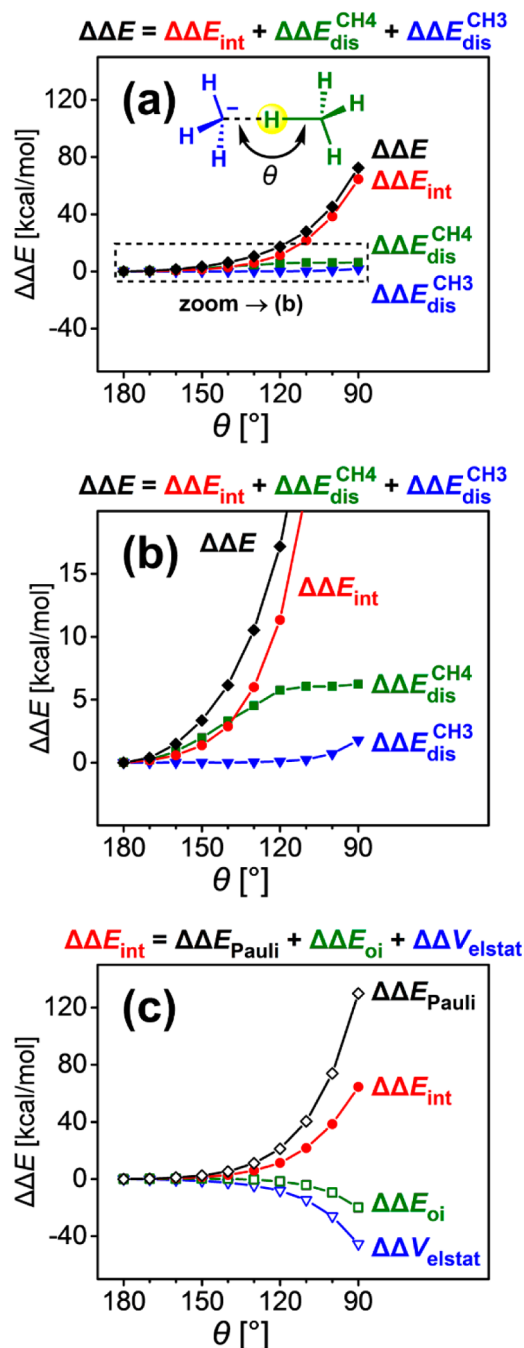
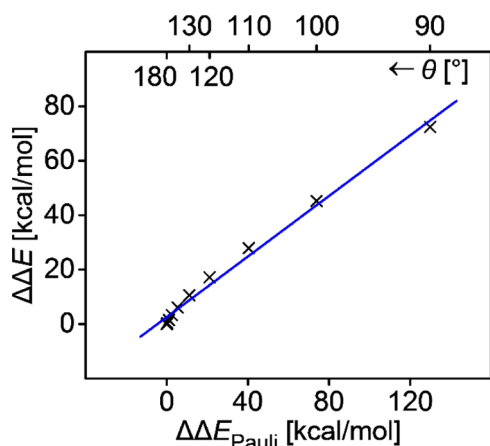


Figure 6. Influence of C⋯H⋯C bond angle on the bond energy of methane and methyl anion in the intermolecular proton transfer transition structure based on the ETS-NOCV analysis.



**Figure 7.** Plot of the relative bond energies ( $\Delta\Delta E$ ) versus the relative Pauli interactions ( $\Delta\Delta E_{\text{Pauli}}$ ).  $\Delta\Delta E = 0.56 \Delta\Delta E_{\text{Pauli}} + 2.6$ ,  $R^2 = 0.99$ .

versus the relative Pauli interactions. The smaller the  $\text{C}\cdots\text{H}\cdots\text{C}$  bond angle is, the shorter the distance between the methane and methyl anion will be, and consequently, stronger repulsive Pauli interaction and higher relative energy will be obtained.

Based on our detailed ETS–NOCV analysis, we concluded that the preference for the linear  $\text{C}\cdots\text{H}\cdots\text{C}$  arrangement is mainly determined by the minimization of the destabilizing HOMO–HOMO interaction while the maximization of the stabilizing HOMO–LUMO interactions plays a relatively less important role. Considering that the summation of Pauli repulsion and electrostatic interaction can be regarded as steric repulsion, our conclusions of this part can also be written as follows: minimization of the steric repulsion between the carbon acid and carbanion results in the linear  $\text{C}\cdots\text{H}\cdots\text{C}$  arrangement of the intermolecular proton transfer transition structure.

**Substituent Effect on Carbanion Translocations.** Next, we focused our attention toward the substituent effect, considering two aspects according to the Marcus theory:<sup>42</sup> first on the intrinsic barriers ( $\Delta E_i^\ddagger$ ) and then the contributions of thermodynamic facts (eq 1). In this part, we used the 1,4-proton transfer as the model reaction system (Table 3). Similar results were obtained for 1,2- and 1,3-proton transfers (see Supporting Information for details).

$$\Delta E^\ddagger = \Delta E_i^\ddagger + \Delta E_{\text{rxn}}/2 + (\Delta E_{\text{rxn}})^2/(16\Delta E_i^\ddagger) \quad (1)$$

**On the Intrinsic Barriers.** As mentioned above, the activation barrier of 1,4-proton transfer in *n*-butyl anion **C** is 18.2 kcal/mol (Table 3, entry 1). Adding electron-withdrawing cyano groups dramatically decreases the activation barrier to 9.0 kcal/mol (Table 3, entry 2). Interestingly, the  $\pi$ -donating but  $\sigma$ -withdrawing halogen atoms show different substituent effects. Chloro substituents lead to a lower reaction barrier (13.9 kcal/mol for anion **I** versus 18.2 kcal/mol for the parent system) and, thus, may accelerate the 1,4-proton transfer (Table 3, entry 3). In contrast, fluoro groups increase the activation barrier to 22.8 kcal/mol and subsequently make the 1,4-carbanion translocation more sluggish than the parent system (Table 3, entry 4). We reasoned that the presence of the electron-withdrawing groups may contract the  $\sigma(\text{C}-\text{H})$  and  $n(\text{C}^-)$  orbitals and, therefore, decrease the Pauli repulsion and reaction barrier. Simultaneously, the existence of a  $\pi$ -donating substituent<sup>43</sup> may increase the Pauli repulsion and slow down the proton transfer. The trade-off between these two opposite

**Table 3.** Substituent Effect on 1,4-Proton Transfer<sup>a</sup>

entry	TS	R	R'	$\Delta E_{\text{rxn}}$	$\Delta E^\ddagger$	$\Delta E_i^{\ddagger b}$
<i>parent system</i>						
1	C → C	H	H	0.0	18.2	18.2
<i>tetrasubstituted</i>						
2	H → H	CN	CN	0.0	9.0	9.0
3	I → I	Cl	Cl	0.0	13.9	13.9
4	J → J	F	F	0.0	22.8	22.8
<i>monosubstituted</i>						
5	K → L	H	CN	-26.6	2.1	11.6
6	M → N	H	Cl	-9.8	11.8	16.3
7	O → P	H	F	-0.9	18.6	19.0

<sup>a</sup>Energies are reported in kcal/mol. rxn = reaction. <sup>b</sup>Intrinsic barriers.

effects results in the dramatically different substituent effect of chloro and fluoro substituents.

**Thermodynamic Contributions.** The Marcus theory connects the thermodynamic and kinetic factors.<sup>42</sup> In most cases, a stronger base (a thermodynamic factor) deprotonates faster (a kinetic problem). In our cases, we may also expect correlations between thermodynamics and kinetics. Adding an electron-withdrawing group on the acidic site will lead to stronger acidity of the  $\text{C}-\text{H}$  bond (lower  $\sigma^*(\text{C}-\text{H})$  orbital energy) and a lower activation barrier. Correspondingly, if we add one electron-withdrawing substituent on the basic site, the proton transfer will become much more difficult. Quantitative analysis using a cyano group as the electron-withdrawing group indicated that the activation barrier for proton transfer between carbons satisfies these discussions (Table 3, entry 5). For the exothermic forward reaction **K** → **L**, the activation barrier is only 2.1 kcal/mol. However, for the endothermic reverse reaction **L** → **K**, the reaction barrier is as high as  $2.1 - (-26.6)$ , i.e., 28.7 kcal/mol. Notably, the intrinsic barrier for the corresponding hypothetical thermoneutral process is calculated to be 11.6 kcal/mol, just between those for the parent systems **C** → **C** (18.2 kcal/mol) and **H** → **H** (9.0 kcal/mol). The same conclusions can be applied to the monochloro substitution case (Table 3, entry 6). However, monofluoro-substituted anion **O** gives a different result (Table 3, entry 7). Although the **O** → **P** process is slightly exothermic ( $\Delta E_{\text{rxn}} = -0.9$  kcal/mol) due to the  $\sigma$ -withdrawing property of the fluoro atom, the reaction barrier is increased as compared to the parent system (18.6 kcal/mol for anion **O** versus 18.2 kcal/mol for the parent system) mainly because of the  $\pi$ -donating character of the fluoro group,<sup>43</sup> which may lead to a larger Pauli repulsion in the transition structure.

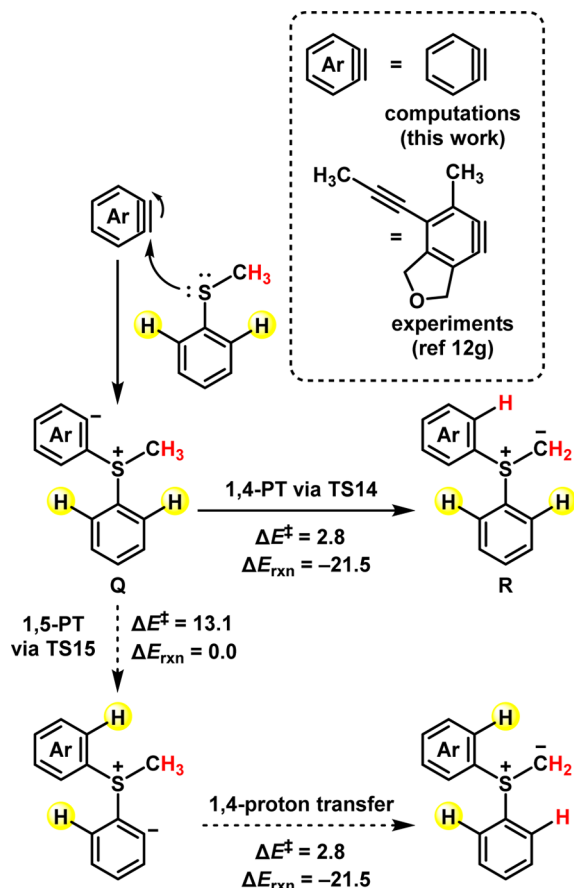
**Regioselectivity. Tethering Effect.** Considering that there may exist multiple reaction centers ( $\text{C}-\text{H}$  bonds) in carbanions, there are regioselectivity issues. In the case of *n*-heptyl anion **F**, theoretically, all direct 1,*n*-proton transfers ( $n = 2-7$ ) may occur. However, the most kinetically favored pathways are 1,5- and 1,6-proton transfers with less ring strains.

**Substituent Effect.** We have shown above that electron-withdrawing groups on the acidic site may induce lower intramolecular proton transfer activation barriers. The relationship between thermodynamic properties (acidity/basicity) and kinetic data (activation barrier) indicated that we can use the readily available thermodynamic data, such as Bordwell's  $\text{p}K_a$

values in DMSO<sup>44</sup> and proton affinities,<sup>45</sup> to predict the relative ease of intramolecular proton transfers with thermodynamic bias.

The 1,4-proton transfer in the generation of sulfur ylide induced by the nucleophilic addition of thioether to aryne was proposed to proceed through an intramolecular process (Scheme 3).<sup>12a,b,g</sup> A labeling experiment by the Hoye group

**Scheme 3. Formation of Sulfur Ylide via 1,4-Proton Transfer<sup>a</sup>**



<sup>a</sup>Energies are reported in kcal/mol.

confirmed that the 1,4-proton transfer indeed takes place in an intramolecular fashion.<sup>12g</sup> And the 1,4-proton abstraction is expected to be much faster than the possible 1,5-proton transfer between the two arenes based on the same experiment; otherwise, a certain amount of H/D scrambling should be observed.

According to our analysis above, intrinsically the 1,5-proton transfer should have a similar (or even lower) activation barrier as the 1,4-one (Table 1). However, our quantum chemical calculations at the SCS-MP2// $\omega$ B97XD level indicated that the highly exothermic 1,4-proton transfer ( $\Delta E_{rxn} = -21.5$  kcal/mol) is much easier than the thermoneutral 1,5-one (2.8 kcal/mol for 1,4-PT versus 13.1 kcal/mol for 1,5-PT). This contradiction is mainly due to the thermodynamic contributions. The  $pK_a$  of S(CH3)3+ in DMSO is 18.2, while that of benzene is above 35 (the  $pK_a$  of DMSO).<sup>44</sup> The large  $\Delta pK_a$  results in the preference for the experimentally observed 1,4-proton transfer. Moreover, considering that the activation barrier for the 1,5-proton transfer is only 13.1 kcal/mol, we

predict that such a process can be achieved if diarylthioethers are used as substrates.

**Direct or Assisted.** According to our calculations, the intrinsic barriers for 1,2- and 1,3-proton transfers are higher than 30 kcal/mol (Table 1,  $n = 2$  and 3), indicating that such processes should be very difficult unless assisted by proton shuttles. Our previous studies on the phosphine-catalyzed (3 + 2) cycloadditions (Scheme 2a) have shown that such a process can be assisted by water molecules through a protonation/deprotonation mechanism.<sup>10a,c</sup> However, we cannot rule out the possibilities that 1,2- and 1,3-proton transfers could occur intramolecularly if these processes are strongly exothermic.

Experimental and computational observations have shown that 1, $n$ -proton transfer with  $n > 3$  may occur intramolecularly (Scheme 2b). We have shown some examples<sup>12</sup> for 1,4-proton transfers in Scheme 2b and discussed one of them (discovered by Hoye group,<sup>12g</sup> Scheme 3) in detail. In these examples, the presence of the electron-withdrawing substituents is crucial in accelerating the intramolecular proton transfer. Carbanion translocations via direct 1,5-proton transfers have also been experimentally verified (Scheme 2b, bottom).<sup>13</sup> The Wang group proposed the feasibility of an intramolecular carbon-to-carbon 1,6-proton transfer in their computational studies<sup>15a</sup> on the phosphine-catalyzed (4 + 2) cycloaddition developed by the Kwon group.<sup>9c</sup> This is consistent with our analysis on the parent system (Table 1,  $n = 6$ ), showing that direct 1,6-proton transfer is generally easy. However, no experiments have been conducted to verify Wang's hypothesis. Considering that the intramolecular nature of 1,6-sigmatropic proton shifts in pentadienyl lithiums has already been experimentally confirmed,<sup>15a</sup> we envision that more examples for direct 1,6-proton transfer in nonconjugated system could be obtained.

## CONCLUSIONS

Based on quantum chemical calculations and ETS–NOCV charge and energy decomposition analyses, we have investigated the translocations of carbanions via 1, $n$ -proton transfers in detail. Generally, the larger the  $n$  is, the easier the intramolecular proton transfer will be. Intramolecular 1,2- and 1,3-proton transfers are difficult and could be facilitated by proton shuttles via the protonation/deprotonation mechanism, whereas direct 1,4- and 1,5-proton transfers are facile in most cases. These observations can be explained by the trade-off between ring strain and stereoelectronic requirement, i.e., the linear  $C\cdots H\cdots C$  displacement in the proton transfer transition structure. The substituent effect was also examined, showing that addition of electron-withdrawing groups will generally decrease the reaction barrier. In contrast,  $\pi$ -donors, such as fluoro groups, induce a higher intrinsic barrier due to larger Pauli repulsive interactions. Thermodynamic contributions were found to play important roles in the regiochemistry. According to the Marcus theory, we can understand and predict the regioselectivity by comparing the difference in intrinsic barriers (mainly controlled by the tether lengths) and  $pK_a$  values. We encourage chemists who are interested in phosphine catalysis, aryne chemistry, and other research areas on carbanions to use our conclusions to rationalize and predict the feasibility of carbanion translocations via intramolecular proton transfers.

## ■ ASSOCIATED CONTENT

### Supporting Information

The Supporting Information is available free of charge on the ACS Publications website at DOI: 10.1021/acs.joc.7b00194.

Benchmark calculations, tunneling effect, additional results of the substituent effect, computed energies, and Cartesian coordinates of all stationary points (PDF)

## ■ AUTHOR INFORMATION

### Corresponding Author

\*E-mail: yuzx@pku.edu.cn.

### ORCID

Zhi-Xiang Yu: 0000-0003-0939-9727

### Notes

The authors declare no competing financial interest.

## ■ ACKNOWLEDGMENTS

We thank the National Natural Science Foundation of China (21232001—Mechanistic Studies of Several Important Organic Reactions) for financial support.

## ■ REFERENCES

- (1) For selected reviews on intramolecular hydride transfers, see: (a) Ahlberg, P.; Jonäll, G.; Engdahl, C. *Adv. Phys. Org. Chem.* **1983**, *19*, 223. (b) Tantillo, D. J. *Nat. Prod. Rep.* **2011**, *28*, 1035. (c) Naredla, R. R.; Klumpp, D. A. *Chem. Rev.* **2013**, *113*, 6905.
- (2) For selected reviews on intramolecular hydrogen atom transfers, see: (a) Wolff, M. E. *Chem. Rev.* **1963**, *63*, 55. (b) Majetich, G.; Wheless, K. *Tetrahedron* **1995**, *51*, 7095. (c) Robertson, J.; Pillai, J.; Lush, R. K. *Chem. Soc. Rev.* **2001**, *30*, 94. (d) Čeković, Ž. *J. Serb. Chem. Soc.* **2005**, *70*, 287. (e) Dénès, F.; Beaufils, F.; Renaud, P. *Synlett* **2008**, 2389. (f) Sperry, J.; Liu, Y.-C.; Brimble, M. A. *Org. Biomol. Chem.* **2010**, *8*, 29. (g) Chiba, S.; Chen, H. *Org. Biomol. Chem.* **2014**, *12*, 4051. (h) Nechab, M.; Mondal, S.; Bertrand, M. P. *Chem. - Eur. J.* **2014**, *20*, 16034.
- (3) For selected reviews on intramolecular proton transfers, see: (a) Formosinho, S. J.; Arnaut, L. G. *J. Photochem. Photobiol., A* **1993**, *75*, 21. (b) Hobza, P.; Šponer, J. *Chem. Rev.* **1999**, *99*, 3247. (c) Crespo-Hernández, C. E.; Cohen, B.; Hare, P. M.; Kohler, B. *Chem. Rev.* **2004**, *104*, 1977. (d) Agmon, N. *J. Phys. Chem. A* **2005**, *109*, 13.
- (4) For recent reviews on proton-coupled electron transfers, see: (a) Weinberg, D. R.; Gagliardi, C. J.; Hull, J. F.; Murphy, C. F.; Kent, C. A.; Westlake, B. C.; Paul, A.; Ess, D. H.; McCafferty, D. G.; Meyer, T. J. *Chem. Rev.* **2012**, *112*, 4016. (b) Migliore, A.; Polizzi, N. F.; Therien, M. J.; Beratan, D. N. *Chem. Rev.* **2014**, *114*, 3381.
- (5) For selected reviews on sigmatropic hydrogen shifts, see: (a) Spangler, C. W. *Chem. Rev.* **1976**, *76*, 187. (b) Houk, K. N.; Li, Y.; Evanseck, J. D. *Angew. Chem., Int. Ed. Engl.* **1992**, *31*, 682.
- (6) For selected examples, see: (a) Lin, X.; Hezari, M.; Koeppe, A. E.; Floss, H. G.; Croteau, R. *Biochemistry* **1996**, *35*, 2968. (b) Williams, D. C.; Carroll, B. J.; Jin, Q.; Rithner, C. D.; Lenger, S. R.; Floss, H. G.; Coates, R. M.; Williams, R. M.; Croteau, R. *Chem. Biol.* **2000**, *7*, 969. (c) Ravn, M. M.; Peters, R. J.; Coates, R. M.; Croteau, R. *J. Am. Chem. Soc.* **2002**, *124*, 6998. (d) Hong, Y. J.; Tantillo, D. J. *Org. Lett.* **2006**, *8*, 4601. (e) Hong, Y. J.; Tantillo, D. J. *J. Am. Chem. Soc.* **2011**, *133*, 18249. (f) Hong, Y. J.; Tantillo, D. J. *J. Am. Chem. Soc.* **2014**, *136*, 2450.
- (7) Surendra, K.; Corey, E. J. *J. Am. Chem. Soc.* **2008**, *130*, 8865.
- (8) Hong, Y. J.; Tantillo, D. J. *J. Am. Chem. Soc.* **2015**, *137*, 4134.
- (9) For selected experimental studies on phosphine-catalyzed reactions involving carbanion translocations, see: (a) Zhang, C.; Lu, X. *J. Org. Chem.* **1995**, *60*, 2906. (b) Lu, X.; Zhang, C.; Xu, Z. *Acc. Chem. Res.* **2001**, *34*, 535. (c) Tran, Y. S.; Kwon, O. *J. Am. Chem. Soc.* **2007**, *129*, 12632. (d) Zhang, Q.; Yang, L.; Tong, X. *J. Am. Chem. Soc.* **2010**, *132*, 2550. (e) En, D.; Zou, G.-F.; Guo, Y.; Liao, W.-W. *J. Org. Chem.* **2014**, *79*, 4456. (f) Yang, L.; Ma, J. *Huaxue Xuebao* **2016**, *74*, 130 and references cited therein.
- (10) For selected computational studies on phosphine-catalyzed reactions involving carbanion translocations, see: (a) Xia, Y.; Liang, Y.; Chen, Y.; Wang, M.; Jiao, L.; Huang, F.; Liu, S.; Li, Y.; Yu, Z.-X. *J. Am. Chem. Soc.* **2007**, *129*, 3470. (b) Mercier, E.; Fonovic, B.; Henry, C.; Kwon, O.; Dudding, T. *Tetrahedron Lett.* **2007**, *48*, 3617. (c) Liang, Y.; Liu, S.; Xia, Y.; Li, Y.; Yu, Z.-X. *Chem. - Eur. J.* **2008**, *14*, 4361. (d) Liang, Y.; Liu, S.; Yu, Z.-X. *Synlett* **2009**, 2009, 905. (e) Zhao, L.; Wen, M.; Wang, Z.-X. *Eur. J. Org. Chem.* **2012**, 2012, 3587. (f) Zheng, L.; Tang, M.; Wang, Y.; Guo, X.; Wei, D.; Qiao, Y. *Org. Biomol. Chem.* **2016**, *14*, 3130.
- (11) For one example of oxygen-to-carbon 1,3-proton transfer in aryne chemistry, see: Willoughby, P. H.; Niu, D.; Wang, T.; Haj, M. K.; Cramer, C. J.; Hoye, T. R. *J. Am. Chem. Soc.* **2014**, *136*, 13657.
- (12) For selected examples of 1,4-proton transfers in aryne chemistry, see: (a) Blackburn, G. M.; Ollis, W. D. *Chem. Commun.* **1968**, 1261. (b) Xu, H.-D.; Cai, M.-Q.; He, W.-J.; Hu, W.-H.; Shen, M.-H. *RSC Adv.* **2014**, *4*, 7623. (c) Swain, S. P.; Shih, Y.-C.; Tsay, S.-C.; Jacob, J.; Lin, C.-C.; Hwang, K. C.; Horng, J.-C.; Hwu, J. R. *Angew. Chem., Int. Ed.* **2015**, *54*, 9926. (d) Roy, T.; Thangaraj, M.; Gonnade, R. G.; Biju, A. T. *Chem. Commun.* **2016**, 52, 9044. (e) Zhang, J.; Chen, Z.-X.; Du, T.; Li, B.; Gu, Y.; Tian, S.-K. *Org. Lett.* **2016**, *18*, 4872. (f) Roy, T.; Thangaraj, M.; Kaicharla, T.; Kamath, R. V.; Gonnade, R. G.; Biju, A. T. *Org. Lett.* **2016**, *18*, 5428. (g) Chen, J.; Palani, V.; Hoye, T. R. *J. Am. Chem. Soc.* **2016**, *138*, 4318. (h) Ross, S. P.; Hoye, T. R. *Nat. Chem.* **2017**, DOI: 10.1038/nchem.2732.
- (13) For 1,5-proton transfers in aryne chemistry, see ref 12h and also: Shi, J.; Qiu, D.; Wang, J.; Xu, H.; Li, Y. *J. Am. Chem. Soc.* **2015**, *137*, 5670.
- (14) (a) Dyker, G., Ed. *Handbook of C–H Transformations: Application in Organic Synthesis*; Wiley-VCH: Weinheim, 2005. (b) Yu, J.-Q.; Shi, Z., Eds. *C–H Activation. Topics in Current Chemistry*; Springer: Berlin, Heidelberg, 2010.
- (15) Sigmatropic proton shifts were not discussed in this study except the simplest 1,2-shift. For selected studies on carbanion translocations via sigmatropic proton shifts, see: (a) Bates, R. B.; Brenner, S.; Deines, W. H.; McCombs, D. A.; Potter, D. E. *J. Am. Chem. Soc.* **1970**, *92*, 6345. (b) Tantillo, D. J.; Hoffmann, R. *Helv. Chim. Acta* **2003**, *86*, 3525.
- (16) For reviews on carbanions in the gas phase, see: (a) Tian, Z.; Kass, S. R. *Chem. Rev.* **2013**, *113*, 6986. (b) Danikiewicz, W.; Zimnicka, M. *Mass Spectrom. Rev.* **2016**, *35*, 123.
- (17) For reports on “naked” carbanions in solution, see: (a) Perrin, C. L.; Reyes-Rodríguez, G. *J. Am. Chem. Soc.* **2014**, *136*, 15263. (b) Lishchynskiy, A.; Miloserdov, F. M.; Martin, E.; Benet-Buchholz, J.; Escudero-Adán, E. C.; Konovalov, A. I.; Grushin, V. V. *Angew. Chem., Int. Ed.* **2015**, *54*, 15289.
- (18) Frisch, M. J.; Trucks, G. W.; Schlegel, H. B.; Scuseria, G. E.; Robb, M. A.; Cheeseman, J. R.; Scalmani, G.; Barone, V.; Mennucci, B.; Petersson, G. A.; Nakatsuji, H.; Caricato, M.; Li, X.; Hratchian, H. P.; Izmaylov, A. F.; Bloino, J.; Zheng, G.; Sonnenberg, J. L.; Hada, M.; Ehara, M.; Toyota, K.; Fukuda, R.; Hasegawa, J.; Ishida, M.; Nakajima, T.; Honda, Y.; Kitao, O.; Nakai, H.; Vreven, T.; Montgomery, J. A., Jr.; Peralta, J. E.; Ogliaro, F.; Bearpark, M.; Heyd, J. J.; Brothers, E.; Kudin, K. N.; Staroverov, V. N.; Kobayashi, R.; Normand, J.; Raghavachari, K.; Rendell, A.; Burant, J. C.; Iyengar, S. S.; Tomasi, J.; Cossi, M.; Rega, N.; Millam, J. M.; Klene, M.; Knox, J. E.; Cross, J. B.; Bakken, V.; Adamo, C.; Jaramillo, J.; Gomperts, R.; Stratmann, R. E.; Yazyev, O.; Austin, A. J.; Cammi, R.; Pomelli, C.; Ochterski, J. W.; Martin, R. L.; Morokuma, K.; Zakrzewski, V. G.; Voth, G. A.; Salvador, P.; Dannenberg, J. J.; Dapprich, S.; Daniels, A. D.; Farkas, Ö.; Foresman, J. B.; Ortiz, J. V.; Cioslowski, J.; Fox, D. J. *Gaussian 09*, Revision D.01; Gaussian, Inc.: Wallingford, CT, 2009.
- (19) Chai, J.-D.; Head-Gordon, M. *Phys. Chem. Chem. Phys.* **2008**, *10*, 6615.
- (20) (a) Krishnan, R.; Binkley, J. S.; Seeger, R.; Pople, J. A. *J. Chem. Phys.* **1980**, *72*, 650. (b) McLean, A. D.; Chandler, G. S. *J. Chem. Phys.*

- 1980, 72, 5639. (c) Clark, T.; Chandrasekhar, J.; Spitznagel, G. W.; Schleyer, P. v. R. *J. Comput. Chem.* **1983**, 4, 294. (d) Frisch, M. J.; Pople, J. A.; Binkley, J. S. *J. Chem. Phys.* **1984**, 80, 3265.
- (21) Neese, F. The ORCA program system. *Wiley Interdiscip. Rev.: Comput. Mol. Sci.* **2012**, 2, 73.
- (22) Møller, C.; Plesset, M. S. *Phys. Rev.* **1934**, 46, 618.
- (23) Grimme, S. *J. Chem. Phys.* **2003**, 118, 9095.
- (24) (a) Dunning, T. H., Jr. *J. Chem. Phys.* **1989**, 90, 1007. (b) Kendall, R. A.; Dunning, T. H., Jr.; Harrison, R. J. *J. Chem. Phys.* **1992**, 96, 6796. (c) Woon, D. E.; Dunning, T. H., Jr. *J. Chem. Phys.* **1993**, 98, 1358.
- (25) (a) Feyereisen, M.; Fitzgerald, G.; Komornicki, A. *Chem. Phys. Lett.* **1993**, 208, 359. (b) Vahtras, O.; Almlöf, J.; Feyereisen, M. W. *Chem. Phys. Lett.* **1993**, 213, 514.
- (26) Weigend, F.; Köhn, A.; Hättig, C. *J. Chem. Phys.* **2002**, 116, 3175.
- (27) ADF2016.106, SCM, Theoretical Chemistry, Vrije Universiteit, Amsterdam, The Netherlands, <http://www.scm.com>.
- (28) (a) Fonseca Guerra, C.; Snijders, J. G.; te Velde, G.; Baerends, E. J. *Theor. Chem. Acc.* **1998**, 99, 391. (b) te Velde, G.; Bickelhaupt, F. M.; Baerends, E. J.; Fonseca Guerra, C.; van Gisbergen, S. J. A.; Snijders, J. G.; Ziegler, T. *J. Comput. Chem.* **2001**, 22, 931.
- (29) Chai, J.-D.; Head-Gordon, M. *J. Chem. Phys.* **2008**, 128, 084106.
- (30) (a) van Lenthe, E.; Baerends, E. J. *J. Comput. Chem.* **2003**, 24, 1142. (b) Chong, D. P. *Mol. Phys.* **2005**, 103, 749.
- (31) Legault, C. Y. *CYLview*, 1.0b; Université de Sherbrooke, 2009. <http://www.cylview.org>.
- (32) GUI 2016, SCM, Amsterdam, The Netherlands, <http://www.scm.com>.
- (33) Quantum tunneling increases the rate constants for intramolecular proton transfers in a magnitude of 10–7000 at 298.15 K, corresponding to a decrease of 1.4–5.2 kcal/mol in terms of Gibbs energy of activation. These results did not change our conclusion that the activation barrier for intramolecular proton transfer decreases with *n*. For details, see [Supporting Information](#).
- (34) (a) Woodward, R. B.; Hoffmann, R. *J. Am. Chem. Soc.* **1965**, 87, 2511. (b) Hoffmann, R.; Woodward, R. B. *Acc. Chem. Res.* **1968**, 1, 17. (c) Woodward, R. B.; Hoffmann, R. *Angew. Chem., Int. Ed. Engl.* **1969**, 8, 781.
- (35) The symmetry-allowed *antarafacial* 1,2-proton shift is geometrically unrealizable. The corresponding transition structure cannot be located.
- (36) (a) Cao, H. Z.; Allavena, M.; Tapia, O.; Evleth, E. M. *J. Phys. Chem.* **1985**, 89, 1581. (b) Latajka, Z.; Scheiner, S. *Int. J. Quantum Chem.* **1986**, 29, 285. (c) Chandra, A. K.; Zeegers-Huyskens, T. *J. Phys. Chem. A* **2005**, 109, 12006.
- (37) For a review on transannular interactions in medium-sized rings, see: Rademacher, P. *Chem. Soc. Rev.* **1995**, 24, 143.
- (38) (a) Mitoraj, M. P.; Michalak, A.; Ziegler, T. *J. Chem. Theory Comput.* **2009**, 5, 962. (b) Mitoraj, M.; Michalak, A.; Ziegler, T. *Organometallics* **2009**, 28, 3727. (c) Kurczab, R.; Mitoraj, M. P.; Michalak, A.; Ziegler, T. *J. Phys. Chem. A* **2010**, 114, 8581. (d) Mitoraj, M. P.; Parafiniuk, M.; Srebro, M.; Handzlik, M.; Buczek, A.; Michalak, A. *J. Mol. Model.* **2011**, 17, 2337.
- (39) Ziegler, T.; Rauk, A. *Theor. Chim. Acta* **1977**, 46, 1.
- (40) (a) Mitoraj, M.; Michalak, A. *J. Mol. Model.* **2007**, 13, 347. (b) Michalak, A.; Mitoraj, M.; Ziegler, T. *J. Phys. Chem. A* **2008**, 112, 1933.
- (41) This approach is closely related to the distortion/interaction or activation strain model; see: (a) Ess, D. H.; Houk, K. N. *J. Am. Chem. Soc.* **2007**, 129, 10646. (b) Ess, D. H.; Houk, K. N. *J. Am. Chem. Soc.* **2008**, 130, 10187. (c) van Zeist, W.-J.; Bickelhaupt, F. M. *Org. Biomol. Chem.* **2010**, 8, 3118. (d) Fernandez, I.; Bickelhaupt, F. M. *Chem. Soc. Rev.* **2014**, 43, 4953.
- (42) (a) Marcus, R. A. *J. Chem. Phys.* **1956**, 24, 966. (b) Marcus, R. A. *Annu. Rev. Phys. Chem.* **1964**, 15, 155. (c) Marcus, R. A. *J. Phys. Chem.* **1968**, 72, 891.
- (43) The  $\pi$ -donating ability of fluoro substituents has been used to explain the torquoselectivity in the electrocyclic ring opening of 3-fluorocyclobutene; see: Dolbier, W. R., Jr.; Koroniak, H.; Houk, K. N.; Sheu, C. *Acc. Chem. Res.* **1996**, 29, 471.
- (44) Bordwell, F. G. *Acc. Chem. Res.* **1988**, 21, 456.
- (45) Bouchoux, G. *Mass Spectrom. Rev.* **2007**, 26, 775.